Journal of Magnetic Resonance 199 (2009) 41–47

Contents lists available at ScienceDirect

Journal of Magnetic Resonance

journal homepage: www.elsevier.com/locate/jmr

Improvements to selective refocusing phased (SERFph) experiments

L. Beguin, N. Giraud, J.M. Ouvrard, J. Courtieu, D. Merlet *

Laboratoire de RMN en milieu orienté, Université Paris-Sud 11, ICMMO, UMR CNRS 8182, Bat. 410, 91405 Orsay cedex, France

ARTICLE INFO

Article history:
Received 28 January 2009
Revised 17 March 2009
Available online 2 April 2009

Keywords:
Selective refocusing
Residual dipolar coupling
NMR in oriented media
Chiral liquid crystal

ABSTRACT

Selective refocusing experiments are very powerful for extracting proton–proton couplings one by one. However we demonstrate in the present work that various spectral artefacts are produced by the initial sequence and we show that the combined addition of a refocusing π pulse and a zero-quantum filter greatly improves the experimental sensitivity, and moreover leads to observation of pure absorption lineshapes in the resulting phased 2D spectrum. These developments are applied to the differentiation of enantiomers dissolved in a chiral liquid crystal.

1. Introduction

The differentiation of enantiomers by NMR is a challenge in organic chemistry [1]. It has been shown how this may be achieved by using a chiral liquid crystal as a solvent, and the most efficient solvents for this purpose are lyotropic liquid crystals obtained by dissolving a synthetic homopolypeptide such as poly-(γ-benzyl)-L-glutamate (PBLG) or poly-(ε-carbobenzoxy)-L-lysin (PCBLL) in a non-denaturing organic co-solvent ($CHCl_3$, CH_2Cl_2, 1,4-dioxane, *N*,*N*-dimethylformamide etc.) [2–8]. In these chiral anisotropic solvents there is a difference in the diastereomeric interactions between the chiral solute and the oriented polypeptide fibers, which produces a difference in their orientational order [9]. Consequently, any anisotropic NMR interaction, such as the dipolar coupling, the chemical shift or the quadrupolar splitting for nuclear spins $I > 1/2$, are different for enantiomers [2–7]. Deuterium NMR has proved to be particularly effective in measuring enantiomeric excess by this method because of the simplicity of the spectra, which are dominated by the large quadrupolar interaction. However, deuterium at natural abundance is an insensitive nucleus for NMR detection, which limits its applications even when using a cryoprobe. Proton NMR has high sensitivity but the spectra of enantiomers in a chiral liquid crystal are often poorly resolved and cannot be used to measure the excess.

Recently, we have developed a new method which simplifies the ^{1}H NMR spectra of molecules dissolved in chiral liquid crystals. This approach, which has been successfully applied to the determination of enantiomeric purity in optically enriched mixtures, uses a homonuclear, selective refocusing, 2D phased experiment (SERFph) [10,11]. But, under certain experimental conditions, the signals in the phased 2D spectrum have a mixed dispersion–absorption line shape which limits the accuracy on the enantiomeric excess determination. In this work, we present different methodological improvements of this sequence to suppress every source of signal distortion.

2. Results and discussion

The SERF sequence, which was initially developed by Fäcke and Berger, is based on the well-known 2D J-resolved experiment [12]. To measure a single proton–proton coupling, the different radiofrequency pulses are semi-selective. The experiment is useful only when the chemical shifts between protons are large compared to the spin–spin total, residual couplings, T_{ij}. Consider the simplest case of two such protons A and X, the first semi-selective, $\pi/2$ pulse is applied at ν_A, the resonance frequency of the only nucleus to be detected in the t_2 acquisition time. After an evolution time $t_1/2$ both A and X nuclei receive semi-selective π pulses and only the desired coupling T_{AX} evolves during the t_1 delay, whereas all the other couplings and the chemical shift are refocused. Unfortunately the phase of the signal is modulated by the coupling during t_1 and thus after a double Fourier transform, the resulting peak shapes are in 'phase-twist'. For this reason, the 2D spectrum is generally processed in magnitude mode. Recently, Nuzillard has shown that a phaseable 2D spectrum can be obtained by using linear prediction toward the negative values of t_1 [13].

The SERFph pulse sequence, which is shown in Fig. 1a, starts as a basic 2D J-resolve sequence, and a *z*-gradient filter is added before t_2, the acquisition [11]. The *z*-filter allows every antiphase single-quantum coherence to defocus, and only retains the in-phase coherences which have evolved during t_1, leading to an improvement in

* Corresponding author. Fax: +33 1 69 15 81 05.
E-mail address: denismerlet@icmo.u-psud.fr (D. Merlet).

1090-7807/$ - see front matter © 2009 Elsevier Inc. All rights reserved.
doi:10.1016/j.jmr.2009.03.012

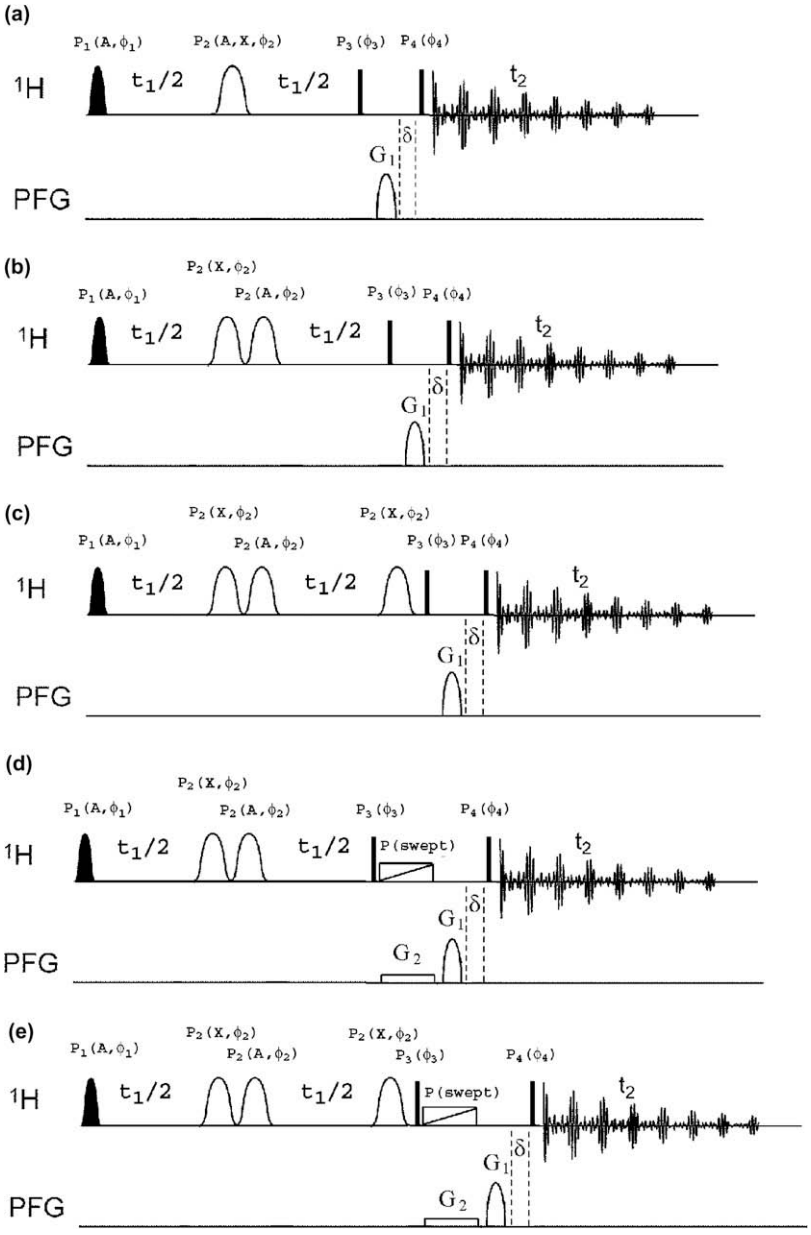

Fig. 1. Pulse sequences for the various SERFph experiments. Pulses $P_i(A,\phi_i)$ or $P_i(X,\phi_i)$ are applied semi-selectively to A or X with phase ϕ_i, $P_2(A,X,\phi_2)$ is applied to A and X simultaneously with phase ϕ_2, $P_i(\phi_i)$ are hard pulses with a phase ϕ_i, P(swept) is a frequency-swept π pulse applied simultaneously with a rectangular z field gradient G_2, G_1 is a z field gradient for the z filter. (a) The definition of the SERFph sequence which corresponds to the appending of one z-gradient filter at the end of a SERF sequence; (b) the sequence b-SERFph with two consecutive selective refocusing π-pulses in place of a single simultaneous π-pulse; (c) the b-SERFph sequence with the addition of a refocusing pulse on X at the end of the evolution time t_1. (d) The b-SERFph sequence with a zero-quantum filter include in the z-gradient filter and (e) the b-SERFph sequence with the both modifications present in the (c and d) SERFph sequences. The black gaussian shapes refer to semi-selective $\pi/2$ pulses; the empty gaussian shapes to semi-selective π pulses and the black sticks to hard $\pi/2$ pulses. The phase cycling is $\phi_1 = x$; $\phi_2 = x,-x$; $\phi_3 = -x,x$; $\phi_4 = x,y,-x,-y$; $\phi_{rec} = x,y,-x,-y$.

resolution. The appending of the z-gradient filter at the end of the sequence generates the following equation for the FID, $S(t_1,t_2)$:

$$S(t_1,t_2) \propto \frac{1}{2}\cos(\pi T_{AX} t_1)\ \{\exp(-i[2\pi\nu_A + \pi T_{AX}]t_2) + \exp(-i[2\pi\nu_A - \pi T_{AX}]t_2)\}, \quad (1)$$

where $T_{AX} = J_{AX} + 2D_{AX}$ is the total coupling between A and X proton spins (J_{AX} and D_{AX} are the scalar and dipolar coupling, respectively).

The signal in t_1 is modulated in amplitude by T_{AX} and, after a double Fourier transform and phase corrections, gives a 2D spectrum in pure absorption.

It has been demonstrated previously that this sequence can greatly simplify the extraction of proton–proton couplings, and allows the measurement of enantiomeric excess from the ^{1}H spectrum of a solution in a chiral liquid crystal solvent [11].

The simultaneous refocusing π pulse on A and X can be achieved with cosine-modulated shaped pulse, whose cosine modulation frequency is one half of the difference between the A and X resonance frequencies. Unfortunately, in this case, the two refocusing pulses correspond to the same *rf* field strength which can limit the applicability of the experiments. In this work we will demonstrate that this refocusing pulse can be applied as two separate, successive, pulses, under some specific experimental conditions, yielding better sensitivity than the initial pulse sequence [14,15].

The SERFph pulse sequence shown in Fig. 1b was tested on the H^3 and H^4 protons of propylene oxide dissolved in a chiral liquid

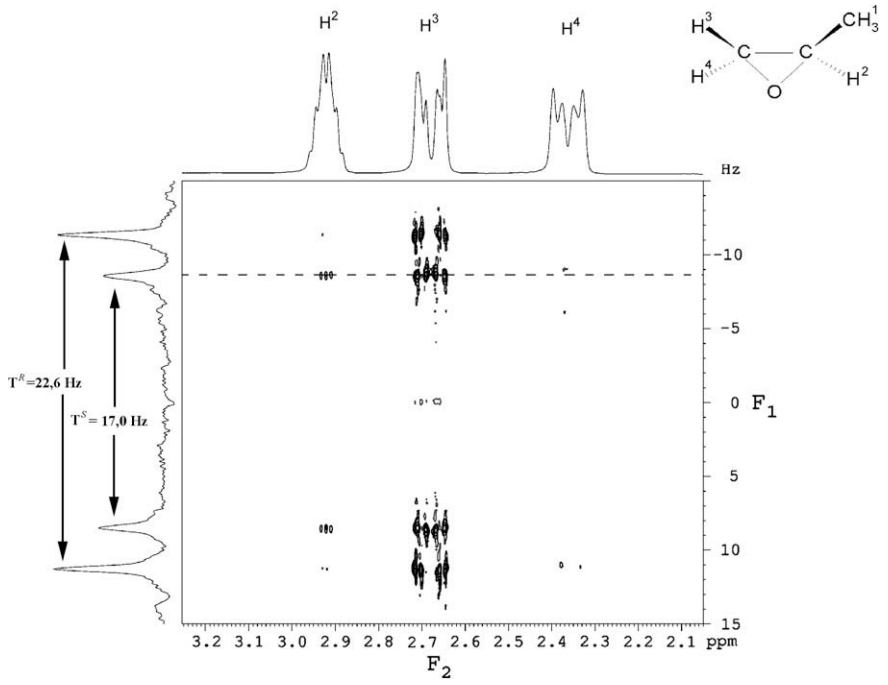

Fig. 2. The SERFph spectrum of propylene oxide dissolved in chiral liquid crystal composed of PBLG and $CDCl_3$ obtained with the sequence 1b. An EBURP2 shaped $\pi 2$ pulse, $P_1(A,\phi_1)$ is applied to the H^3 proton and the offsets of the two REBURP shaped π pulses, $P_2(A,\phi_2)$, $P_2(X,\phi_2)$, are set at H^4 and H^3 proton resonance frequencies, respectively. The projection of the columns is shown along the F_1 dimension (left) and a part of the standard proton spectrum is shown along the F_2 dimension (top). $T^R = T^R_{3,4}$ and $T^S = T^S_{3,4}$.

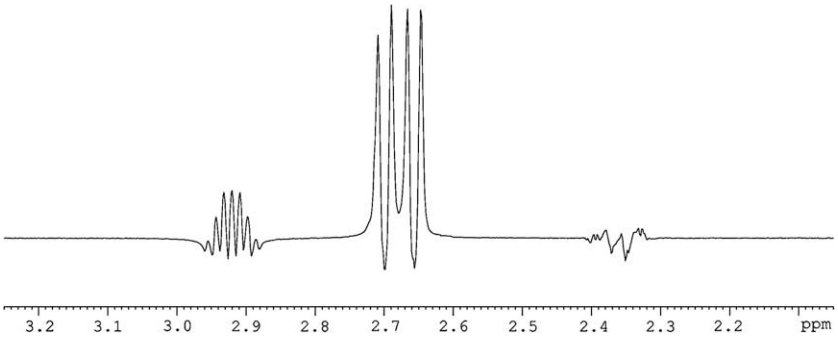

Fig. 3. A row of the SERFph spectrum presented as dashed line in Fig. 2.

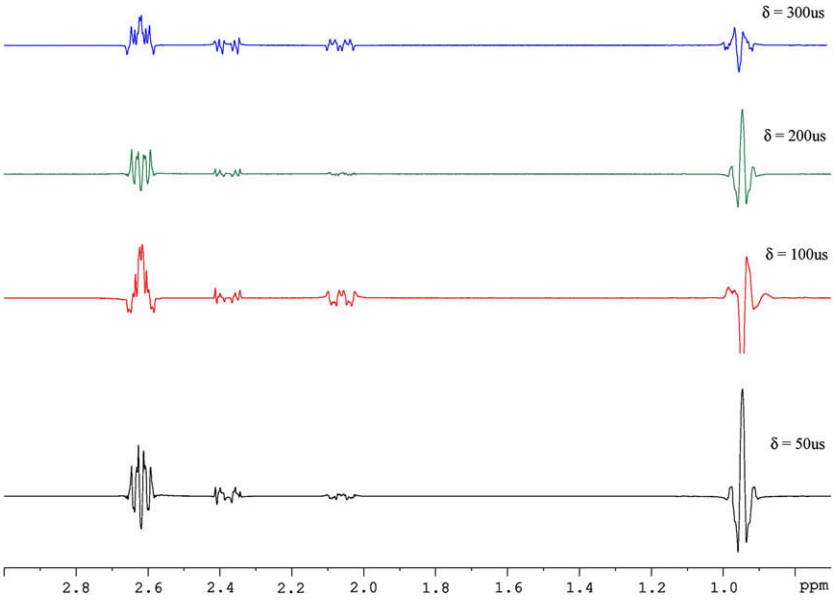

Fig. 4. The influence of the variation in duration of the delay δ on the 1D proton spectrum obtained by using the pulse sequence in Fig. 1a with a fixed value of t_1.

crystal composed of PBLG and $CDCl_3$. The shape of the semi-selective $\pi/2$ and π pulses used are E-BURP2 and RE-BURP, respectively, [16].

The semi-selective $\pi/2$ pulse, $P_1(A,\phi_1)$, has been applied at H^3 proton resonances. The 2D spectrum (Fig. 2) obtained shows clearly the benefit of this experiment in that the total coupling between protons 3 and 4 in the two enantiomers, $T^R_{3,4}$ and $T^S_{3,4}$ are easily obtained from the F_1 projection.

However, the row which is extracted from the H^3 multiplet (Fig. 3) shows that both absorption and dispersion signals contribute to the overall lineshape.

In order to understand which processes occur during the pulse sequence, it is necessary to consider at least a spin system AMX of three coupled protons. The coherences of proton A in term of product operators which will give a detectable signal are modulated as follows just before the z-gradient filter:

$$\begin{aligned}&\mathbf{A}_y \cdot \cos(\pi T_{AX} t_1) \cdot \cos(\pi T_{AM}\Delta) \cdot \cos(2\pi \nu_A \Delta)\\ &\quad + \mathbf{2A}_x\mathbf{M}_z \cdot \cos(\pi T_{AX} t_1) \cdot \sin(\pi T_{AM}\Delta) \cdot \cos(2\pi \nu_A \Delta)\\ &\quad + \mathbf{2A}_x\mathbf{X}_z \cdot \sin(\pi T_{AX} t_1) \cdot \cos(\pi T_{AM}\Delta) \cdot \cos(2\pi \nu_A \Delta)\\ &\quad - \mathbf{4A}_y\mathbf{M}_z\mathbf{X}_z \cdot \sin(\pi T_{AX} t_1) \cdot \sin(\pi T_{AM}\Delta) \cdot \cos(2\pi \nu_A \Delta),\end{aligned} \tag{2}$$

where $\mathbf{A}_y$ corresponds to in-phase single-quantum coherence, $\mathbf{2A}_x\mathbf{M}_z$, $\mathbf{2A}_x\mathbf{X}_z$, $\mathbf{4A}_y\mathbf{M}_z\mathbf{X}_z$ correspond to anti-phase single-quantum coherence. Δ is the duration of the $P_2(X,\phi_2)$ refocusing semi-selective pulse acting on the X nucleus.

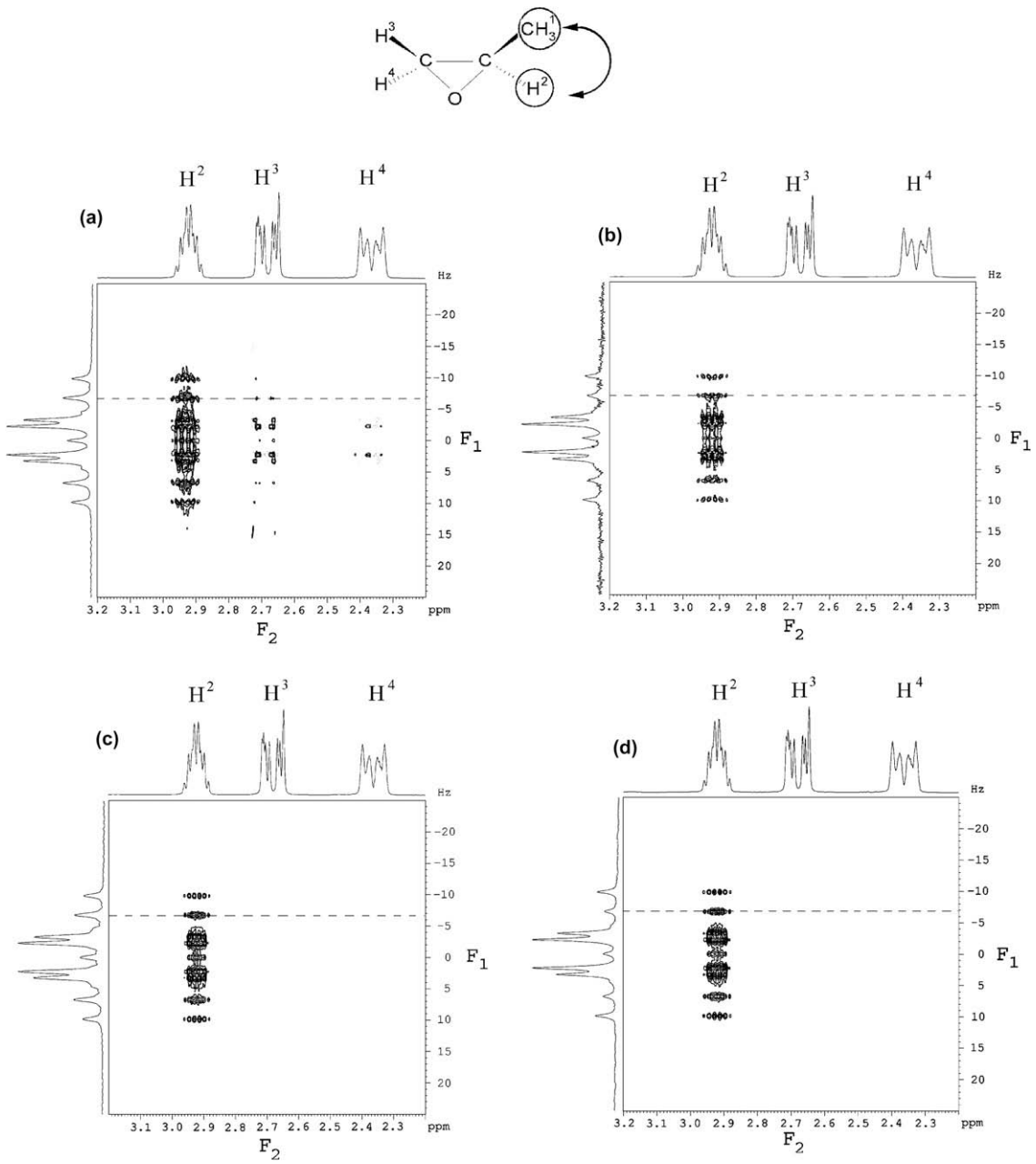

Fig. 5. The 2D SERFph spectra of epoxy propane obtained with different pulse sequences. The spectra a–d were, respectively, acquired by using the pulse sequences 1.b, 1.c, 1.d and 1.e. The semi-selective $\pi/2$ pulse is applied to the proton H^2 resonance, and the semi-selective π pulse on the X nucleus is applied to protons H^1 resonance of the methyl group.

From this result, two conclusions can be made:

(1) The modulation of the operator $\mathbf{A}_y$ demonstrates that the coherences evolve during the refocusing π pulse $P_2(\mathrm{X},\phi_2)$ on the X nucleus under the effect of both the couplings and the chemical shift.

(2) The terms $\mathbf{2A}_x\mathbf{M}_z$, $\mathbf{2A}_x\mathbf{X}_z$, $\mathbf{4A}_y\mathbf{M}_z\mathbf{X}_z$ will generate zero-quantum coherences under the action of $P_3(\phi_3)$ the first non selective $\pi/2$ pulse and are insensitive to the z-gradient filter, and thus will modulate the phase of the final signal.

This second point can be confirmed by varying the delay δ between the gradient of the z-gradient filter and $P_4(\phi_4)$, as illustrated in Fig. 4. A series of 1D spectra obtained by using a classic SERFph sequence with a constant t_1 value shows that the phases of each multiplet depend on δ.

We thus propose two improvements of this sequence:

(1) Evolution during Δ, the length of the refocusing π pulse $P_2(\mathrm{X},\phi_2)$ can be eliminated through symmetrisation of the pulse sequence in t_1, by inserting a second, semi-selective π pulse on X, $P_2(\mathrm{X},\phi_2)$ just before the z-gradient filter [17]. The resulting pulse sequence is shown in Fig. 1c. Thus, before the action of a z-gradient filter, the terms contributing to the observed signal satisfy the following expression:

$$\mathbf{A}_y \cdot \cos(\pi T_{AX} t_1) + \mathbf{2A}_x\mathbf{X}_z \cdot \sin(\pi T_{AX} t_1). \quad (3)$$

The coherences which have evolved during the first π pulse $P_2(\mathrm{X},\phi_2)$ are refocused, but the antiphase term $\mathbf{A}_x\mathbf{X}_z$ remains and will yield a zero-quantum coherence after the $\pi/2$ pulse $P_3(\phi_3)$. The presence of this coherence will cause once again a phase modulation of the final signal.

(2) To suppress the zero-quantum coherence during the filtering period, we add a zero-quantum filter, which was initially proposed by Thrippleton and Keeler [18]. A frequency-swept π pulse P(swept) is applied simultaneously with a z field gradient G_2 (see Fig. 1d). Applying this resulting pulse sequence to the proton A of the AMX spin system, the only term that contributes to the final signal after the zero-quantum filter is:

$$\mathbf{A}_y \cdot \cos(\pi T_{AX} t_1) \cdot \cos(\pi T_{AM} \Delta) \cdot \cos(2\pi \nu_A \Delta). \quad (4)$$

Note that the antiphase coherences are dephased by the zero-quantum filter, whereas the in-phase coherences, $\mathbf{A}_y$, lead to a detected signal. The lineshape of the multiplets from the A nucleus should thus be in absorption, but their intensities will still be modulated by the evolution of the chemical shift and of the couplings during the π pulse $P_2(\mathrm{X},\phi_2)$ on the X nucleus.

In order to maximize the sensitivity of this experiment and obtain a pure phased 2D map, we have combined the two improvements presented above, namely the introduction of a second refocusing π pulse on the X nucleus before the z-gradient filter and the addition of a zero-quantum filter in the z-gradient filter, leading to a zero-quantum z-gradient filter. The resulting pulse sequence is shown in Fig. 1e. The detected signal for this experiment on the AMX system is now given by Eq. (1).

These different experiments were applied to epoxy propane dissolved in a chiral liquid crystal composed of PBLG and $CDCl_3$. Fig. 5 shows the different 2D spectra which were obtained. In all these experiments, the offsets of the soft pulses were set so that the magnetization of the spin of the proton H^2 is initially polarized, and their couplings with the protons H^1 from the methyl group are selected. The F_1 projections of each of these 2D spectra show two quartets, one per enantiomer, at the resonance frequency of H^2. In the first spectrum (Fig. 5a) the presence of many artefacts witnesses the imperfections of the sequence. The spectra shown in Fig. 5b and c are of a better quality either because of the refocusing of the evolution during the first semi-selective π pulse $P_2(\mathrm{X},\phi_2)$ on X (Fig. 5b), or the absence of zero-quantum coherences during the period of filtering (Fig. 5c). However the lineshapes of the F_1 projections are still distorted, illustrating that both improvements are necessary to obtain pure absorption phaseable multiplets.

Finally, a comparison between (i) the spectrum acquired by means of the initial SERFph experiment where only the simultaneous π pulse, $P_2(\mathrm{A},\mathrm{X},\phi_2)$, centered in t_1 was replaced by two separate π pulses $P_2(\mathrm{A},\phi_2)$ and $P_2(\mathrm{X},\phi_2)$ (see the Figs. 1b and 5a) and (ii) that obtained by using the version of SERFph which takes into account the whole of the suggested modifications (see the Figs. 1e and 5d), highlights a clear improvement of spectral quality in that the correct relative intensities are obtained in the F_1 projection.

The gain in sensitivity as well as the lineshapes enhancement can be evaluated by extracting a row from each 2D spectrum (Fig. 6).

On the first row (Fig. 6a), on account of the presence of zero-quantum coherences during the z-gradient filter, the signal is

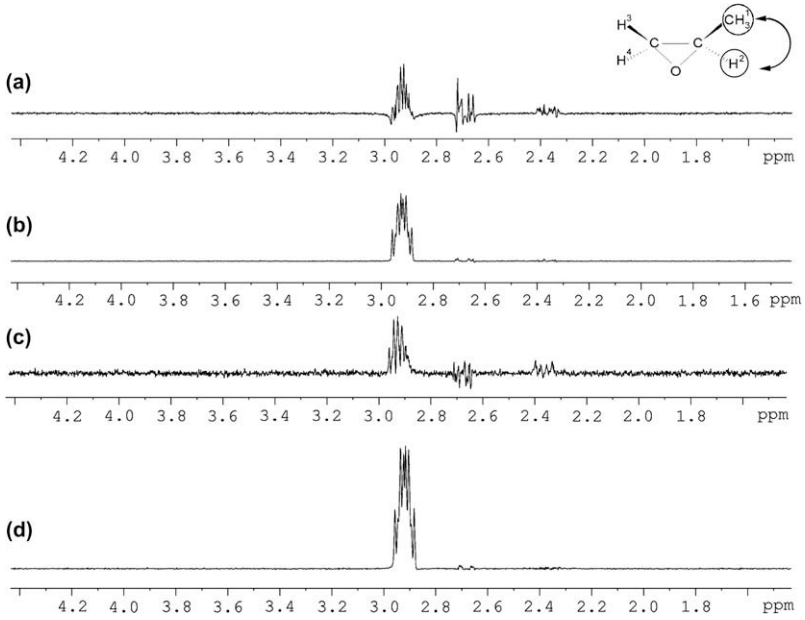

Fig. 6. The same row, symbolised by a dashed line in the 2D spectra, is extracted from the spectra (a–d) presented in Fig. 5.

partly in dispersion and artefacts appear clearly on the signals of the other protons. This is partially eliminated by the introduction of the third semi-selective π pulse before the z-gradient filter (Fig. 6b). We also observe in Fig. 6c that the suppression of zero-quantum coherences has a dramatic effect on the intensity of the signal. Finally, the combined addition of a third refocusing π pulse, and of a zero-quantum z-gradient filter lead to a spectacular enhancement of the sensitivity which is clearly visible on the row in Fig. 6d. Note that as the pulse sequence uses three soft pulses, the duration of the pulse sequence is increased which can be problematic for short relaxation times.

The robustness of this enhanced pulse sequence (Fig. 1e) is demonstrated through the various 2D spectra recorded in order to measure the coupling between the protons H^3 and H^4 with an initial polarization on H^3 (Fig. 7).

A significant improvement in the lineshapes in the F_1 projection of Fig. 7d compared to a which is a consequence of both the incorporation of the second refocusing pulse on the X nucleus and conversion of the z-gradient filter into a zero-quantum z-gradient filter. Note that in Fig. 7c, the signal of only one enantiomer appears, because the zero-quantum coherences involving T_{AM} evolve during the semi-selective X pulse (Eq. (4)), leading to the cancellation of the signal of one enantiomer. Note that if a semi-selective z-gradient filter was used, then zero-quantum coherences would not be created.

It is known that during the semi-selective pulses coherence transfers occur and it is interesting to compare this transfer when using either simultaneous or two separate and consecutive pulses. Preliminary simulation results show that sequential pulses yield better refocalisation compare to simultaneous ones. This work is currently under way.

3. Conclusions

Selective refocusing experiments are very powerful for extractions of the different proton–proton couplings in first order spectra. This is especially important when using proton NMR to distinguish between enantiomers dissolved in chiral liquid crys-

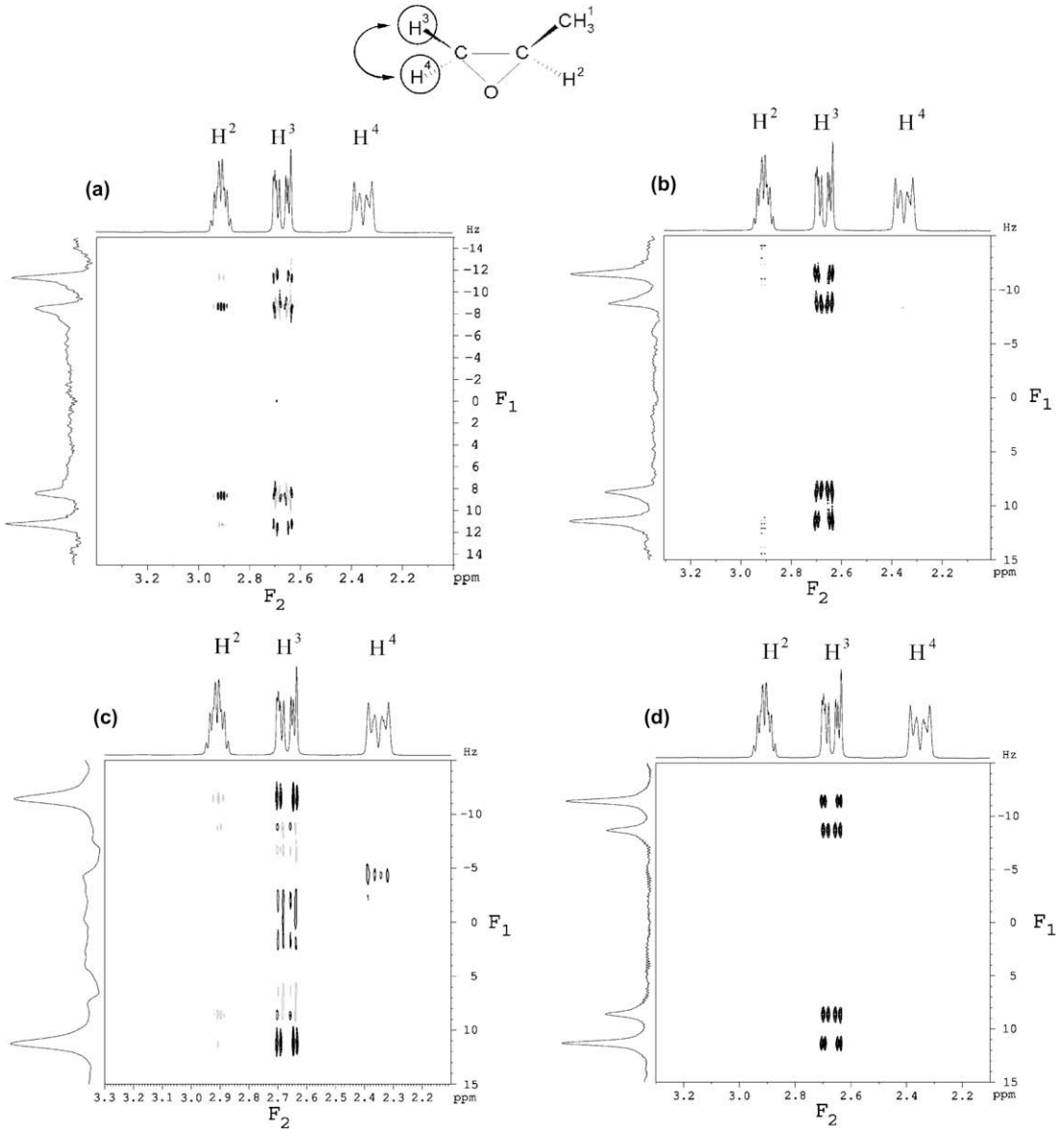

Fig. 7. Spectra (a–d) were, respectively, acquired by using the pulse sequences in Fig. 1b–e. The semi-selective $\pi/2$ pulse is applied to the proton H^3 resonance, and the semi-selective π pulse on X nucleus is applied to the proton H^4 resonance.

tals. We demonstrate in this work that different artefacts are inherent to the initial sequence when consecutive semi-selective refocusing pulses are used. First, the signal is modulated by the evolution during the semi-selective pulse on the X nucleus. Second, zero-quantum coherences evolve during the *z*-gradient filter. These two effects produce a phase-twisted signal. To improve the sensitivity and to obtain pure absorption lineshapes in the phased 2D map, it is necessary to add a refocusing π pulse and a zero-quantum filter.

4. Experimental section

4.1. Sample preparation

Liquid-crystalline NMR sample was prepared using a standard procedure [3]. PBLG was purchased from Sigma and used without further purification. The sample of propylene oxide (purchased from Sigma) was made of 100 mg of PBLG (DP = 782, Sigma), 20.8 mg and 31.9 mg of *R* and *S* enantiomers, and 695 mg of $CDCl_3$. The sample was centrifuged back and forth until an optically homogenous phase was obtained.

4.2. NMR spectroscopy

All the spectra were recorded on a high-resolution Bruker Avance 400 spectrometer (9.4 T) equipped with a QXO probe with a *z* field-gradient coil. The temperature was controlled at 298 K by a standard variable-temperature unit (BVT 3000). The SERFph experiments were recorded using a data matrix of 2048 $(t_2) \times 512$ (t_1) with four scans *per* t_1 increment using the Quadrature Sequential Mode. The relaxation delays were 2 s. The spectral width in F_1 was 50 Hz. The large number of t_1 increment is necessary to take advantage of the great narrowing of the lines in the F_1 dimension.

A zero filling to 1024 data points was applied in t_1 and no filtering was applied prior to double Fourier transform. Signals were phased in both dimensions.

Selective excitations used for the $\pi/2$ and π shaped pulse are EBURP-2 and RE-BURP types [16]. The duration of the RE-BURP refocusing pulse and the E-BURP excitation pulse was 70 ms corresponding to a frequency width of 60 Hz. Other experimental details will be found in the figure captions. For the zero-quanta suppression, the chirp pulse, which was calibrated according to the recommendations of Trippleton and Keeler [18], has a duration of 30 ms and was swept through 40 kHz. The G_1 and G_2 gradient strengths were 10% and 5% of the maximum, respectively. The delay δ was 0.5 ms.

Acknowledgments

The authors thank Dr. Sylvian Cadars for helpful discussions and Prof. James. W. Emsley for helpful corrections.

References

[1] [a] D. Parker, NMR determination of enantiomeric purity, Chem. Rev. 91 (1991) 1441–1457;
[b] R. Rothchild, NMR methods for determination of enantiomeric excess, Chirality 5 (2000) 451–471.
[2] I. Canet, J. Courtieu, A. Loewenstein, A. Meddour, J.M. Péchiné, Enantiomeric analysis in polypeptide lyotropic liquid crystal by deuterium NMR, J. Am. Chem. Soc. 117 (1995) 6520–6525.
[3] M. Sarfati, P. Lesot, D. Merlet, J. Courtieu, Theoretical and experimental aspects of enantiomeric differentiation using natural abundance multinuclear NMR spectroscopy in chiral polypeptide liquid crystals, Chem. Commun. 61 (2000) 2069–2081.
[4] C. Aroulanda, M. Sarfati, J. Courtieu, P. Lesot, Investigation of enantioselectivity of three polypeptide liquid-crystalline solvents using NMR spectroscopy, Enantiomer 6 (2001) 281–287.
[5] A. Meddour, P. Berdagué, A. Hedli, J. Courtieu, P. Lesot, Proton-decoupled carbon-13 NMR spectroscopy in a lyotropic chiral nematic solvent as an analytical tool for the measurement of the enantiomeric excess, J. Am. Chem. Soc. 119 (1997) 4502–4509.
[6] D. Merlet, B. Ancian, J. Courtieu, P. Lesot, Two-dimensional deuterium NMR spectroscopy of chiral molecules oriented in a polypeptide liquid crystal: applications for the enantiomeric analysis through natural abundance deuterium NMR, J. Am. Chem. Soc. 121 (1999) 5249–5258.
[7] M. Jakubcova, A. Meddour, J.M. Pechiné, A. Baklouti, J. Courtieu, Measurement of the optical purity of fluorinated compounds using proton decoupled ^{19}F NMR spectroscopy in a chiral liquid crystal solvent, J. Fluorine Chem. 86 (1997) 149–153.
[8] B. Bikash, R.P. Uday, N. Suryaprakash, Enantiomeric discrimination by double quantum excited selective refocussing (DQ-SERF) experiment, J. Phys. Chem. B 111 (2007) 12403–12410.
[9] J.W. Emsley, P. Lesot, D. Merlet, The orientational order and conformational distributions of the two enantiomers in a racemic mixture of a chiral, flexible molecule dissolved in a chiral nematic liquid crystalline solvent, Phys. Chem. Chem. Phys. 3 (2004) 522–530.
[10] J. Farjon, D. Merlet, P. Lesot, J. Courtieu, Enantiomeric excess measurements in weakly oriented chiral liquid crystal solvents through 2D ^1H selective refocusing experiments, J. Magn. Reson. 158 (2002) 169–172.
[11] J. Farjon, L. Ziani, L. Beguin, D. Merlet, J. Courtieu, Selective NMR excitations in chiral analysis, Annu. Rep. NMR 61 (2007) 283.
[12] T. Fäcke, S. Berger, SERF, a new method for H, H spin-coupling measurement in organic chemistry, J. Magn. Reson. 113 (1995) 114–116.
[13] J.M. Nuzillard, Biselective refocusing pulses and the SERF experiment, J. Magn. Reson. 187 (2) (2007) 193–198.
[14] F. Rastrelli, A. Bagno, Selective J-resolved spectra: a double pulsed field gradient spin–echo approach, J. Magn. Reson. 182 (2006) 29–37.
[15] T. Parella, F. Sanchez-Ferrando, A. Virgili, A simple approach for ultraclean multisite selective excitation using excitation sculpting, J. Magn. Reson. 135 (1998) 50–53.
[16] H. Geen, R. Freeman, Band-selective radiofrequency pulses, J. Magn. Reson. 93 (1991) 93–141.
[17] .S. Cadars, A. Lesage, N. Hedin, B.F. Chmelka, L. Emsley, Selective NMR measurements of homonuclear scalar couplings in isotopically enriched solids, J. Phys. Chem. B 110 (34) (2006) 16982–16991.
[18] M.J. Thrippleton, J. Keeler, Elimination of zero quantum interference in two-dimensional NMR spectra, Angew. Chem. Int. Ed. 42 (2003) 3938–3941.